Test of isospin purity in the $A=42$ isobaric analogs

J. N. Orce,[1,*] P. Petkov,[2,3] C. J. McKay,[1] S. N. Choudry,[1] S. R. Lesher,[1] M. Mynk,[4] D. Bandyopadhyay,[1] S. W. Yates,[1,4] and M. T. McEllistrem[1]

[1]*Department of Physics and Astronomy, University of Kentucky, Lexington, Kentucky 40506, USA*
[2]*Institute for Nuclear Research and Nuclear Energy, Sofia 1784, Bulgaria*
[3]*Institut für Kernphysik der Universität zu Köln, 50937 Köln, Germany*
[4]*Department of Chemistry, University of Kentucky, Lexington, Kentucky 40506, USA*

(Received 10 May 2004; published 23 July 2004)

A careful measurement of the lifetime of the first $2^+_{T=1}$ state in ^{42}Sc has allowed an accurate experimental test of isospin purity in the $A=42$ isobaric analogs by using the isospin formalism. A lifetime of 69 (18) fs has been determined, giving an isoscalar matrix element of 6.8 (8) W.u. Previous measurements of the lifetimes in the mirror nuclei ^{42}Ca and ^{42}Ti provided an isoscalar matrix element of 7.1 (5) W.u. which is very close to the presently measured value for ^{42}Sc.

DOI: 10.1103/PhysRevC.70.014314 PACS number(s): 21.10.Hw, 23.20.Js, 24.10.Lx, 24.80.+y

I. INTRODUCTION

Understanding nuclear symmetries is one of the principal goals in nuclear structure physics. In particular, considerable work has previously been done in order to test charge symmetry on pairs of mirror nuclei, showing that masses [1] and excitation energies [2,3] of mirror pairs agree with the calculated Coulomb energy differences.

A further sensitive test for charge independence of the nuclear force or isospin purity comes through comparisons of the $E2$ transition strengths to the $2^+_{T=1}$ levels in isobaric analogs. Following the theoretical work by Bernstein, Brown, and Madsen [4] and the experimental work of Cottle *et al.* [5,6], one could test isospin purity by comparing the isoscalar matrix elements extracted from the two nuclides with $T_z=\pm 1$ with that extracted from the $T_z=0$ nuclide. In fact, this would test the degree to which the approximate charge independence of nuclear force leads to the same isoscalar matrix elements. That charge independence is only an approximate symmetry is well known from the fact that n-n or p-p low energy scattering lengths are approximately -17 fm, whereas the n-p scattering length is approximately -23 fm [8]. The comparisons provided by Cottle *et al.* [6], and recent measurements [7] for ^{18}Ne show that isospin symmetry is nonetheless conserved for $T=1$ triplets up to $A=30$, but deviations from symmetry are observed for $A=34$, 38, and 42. The transition strength from or to the $2^+_{T=1}$ level is given by the proton multipole matrix element, which is defined in terms of the reduced matrix element as

$$M_p = [(2J_i+1)B(E2;J_i \rightarrow J_f)]^{1/2}. \tag{1}$$

The relationship between matrix elements in the neutron or proton isospin representation yields [4]

$$M_{n(p)}(T_z) = \frac{1}{2}[M_0(T_z) \pm M_1(T_z)], \tag{2}$$

where the positive sign is for neutrons and the negative for protons. $M_0(T_z)$ is the isoscalar multipole matrix element and $M_1(T_z)$ is the isovector multipole matrix element. The assumption of isospin conservation, i.e., charge independence of the nuclear force, implies the following relationships between matrix elements in different isobars:

$$M_0(T'_z) = M_0(T_z), \tag{3}$$

$$M_1(T'_z) = M_1(T_z)\frac{T'_z}{T_z}. \tag{4}$$

In mirror nuclei, $T'_z=-T_z$ and from Eqs. (2)–(4) the relation between proton and isoscalar matrix elements is obtained

$$M_0(T_z) = M_p(T_z) + M_p(-T_z), \tag{5}$$

which implies that for a transition between $T=1$ states in a $T_z=0$ nucleus:

$$M_0(T=1) = 2M_p(T_z=0). \tag{6}$$

Therefore, given the assumption of isospin symmetry, the value of M_0 extracted from the M_p values in two mirror $T_z=\pm 1$ nuclei should be equal, within experimental uncertainties, to the value $M_0=2M_p$ obtained for the $0^+_{T=1}\rightarrow 2^+_{T=1}$ transition in the $T_z=0$ nucleus [4]. This relationship makes an experimental test of isospin purity possible for the isobaric analogs with $A=4n+2$, where n is an integer.

As noted above, Cottle *et al.* [5] have used this formalism to suggest the possibility of the symmetry being broken for $A=34$, 38, and 42 nuclei. The present experiment adds evidence for the triad of nuclei with $A=42$. Cottle *et al.* measured the strength of the $0^+_{gs}\rightarrow 2^+_1$ transitions using the techniques of Coulomb excitation and lifetime measurements [6,7,9]. We have measured the lifetime of the first state in ^{42}Sc using the Doppler-shift attenuation method (DSAM) and line-shape analysis. More precise measurements might be expected because of advances of both experimental tech-

*Electronic address: jnorce@pa.uky.edu; URL: http://www.pa.uky.edu/~jnorce

niques (HPGe and BGO detectors) and the development of lifetime analysis methods [13,14]. Lifetimes in ^{42}Sc were previously measured in 1971 by DSAM, using the ^{40}Ca(^{3}He,$p\gamma$)^{42}Sc reaction at beam energies of 8.4 and 8.6 MeV [15]. This reaction visibly populates states up to 3.9 MeV. Lifetimes were extracted by measuring the centroid position of shifted peaks in coincidence with protons. The measured lifetime τ=100(30) fs for the first $2^+_{T=1}$ state yields a value for the isoscalar matrix element of M_0 =5.7 (9) W.u. presenting a large uncertainty for comparison with the isoscalar matrix element determined from the mirror nuclei, M_0=7.1 (5) W.u.

II. EXPERIMENTAL DETAILS

To populate the $2^+_{T=1}$ state at 1586 keV in ^{42}Sc, we used the ^{42}Ca(^{3}He,$p\gamma$)^{42}Sc reaction (Q=4.9 Mev) at beam energies of 4.2 and 5.1 MeV. The ^{3}He beam was provided by the 7 MV accelerator at the University of Kentucky. Two Ca targets were prepared by evaporating natural Ca onto Ta foils. Their thicknesses were 0.98 and 0.62 mg/cm^2 for the 4.2 and 5.1 MeV experiments, respectively. Argon gas was used to minimize the oxidation of the Ca target during transport to the beam-line chamber. The cross sections measured for different channels of the calcium and oxygen reactions indicate a maximum of 3% oxidation in the targets. The recoiling ^{42}Sc nuclei are predicted to stop inside the Ca target in a layer of $\sim$0.11 mg/cm^2 and after about 1.4 ps. Pulsed-beam techniques were used to reduce background, with beam pulses separated by 533 ns and bunched to about 1.5 ns. This allowed the use of the time-of-flight technique for background suppression by gating on the appropriate prompt time windows [16]. The γ-rays deexciting the nuclei recoiling with an initial velocity of v/c=0.004 were detected using a BGO Compton-suppressed 50% HPGe spectrometer with 2.0 keV resolution. Spectra were taken at angles of 0°, 20°, 37°, 54°, 129°, and 147° with respect to the beam axis for the 4.2 MeV measurement, and 55° and 125° for the 5.1 MeV.

The beam energy of 4.2 MeV was chosen to provide adequate statistics on relevant γ-ray yields while minimizing the side feeding. Even this (relatively) low bombarding energy leaves the nucleus at an excitation energy of above 7 MeV, although the Coulomb barrier for emitted protons would mean that very little excitation would occur above 4 MeV. Figure 1 shows a partial decay scheme including the levels of interest. Only 11% of the deexcitation intensity of the 1586 keV, $2^+_{T=1}$ level could be identified as coming from observed higher-lying levels. This intensity information was obtained at 54° and the partial spectrum is shown in Fig. 2 which also shows that the deexcitation intensity increases with increasing bombarding energy. The γ rays depopulating these levels above the 1586 keV state do not show Doppler-shifted shapes. The line-shape analysis (see below) strongly indicates two main feeding paths, one very fast, and the other slow. The code PACE2 [17], a Monte Carlo simulation for fusion-evaporation reactions, was used to calculate proton emission spectra, which were employed to take into account the alteration of the recoil velocity distributions. The use of PACE2 is supported by previous work [10–12], where, from

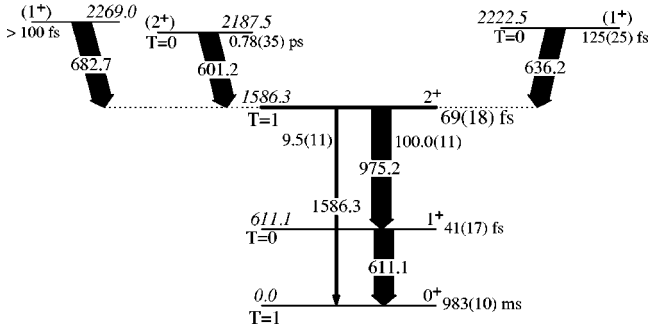

FIG. 1. A ^{42}Sc partial level scheme. The widths of the arrows are proportional to the relative intensities of the transitions depopulating each level. In particular, the relative intensities of the 975 and 1586 keV transitions were previously measured by Kikstra *et al.* [19] as 100.0±1.1 and 9.5±1.1, respectively.

experimental angular correlation and angular distribution of protons from the (^{3}He,p) reaction, it was concluded that the reaction proceeds predominantly through the compound nucleus mechanism up to about $E_{^3\mathrm{He}}$=8 MeV. The additional data taken at 5.1 MeV bombarding energy allowed tests of the accuracy of these corrections since the feeding paths and the proton emission spectra at this energy are different from those at 4.2 MeV. In order to accumulate adequate statistics, the experimental runs at the two incident energies required 14 days of beam time.

III. DATA ANALYSIS

Line-shape analysis [13,14,18] with the inclusion of the calculated side-feeding paths [17] for the (^{3}He,p) reaction has been used for determining lifetimes. This method employs a realistic description of the stopping process of the

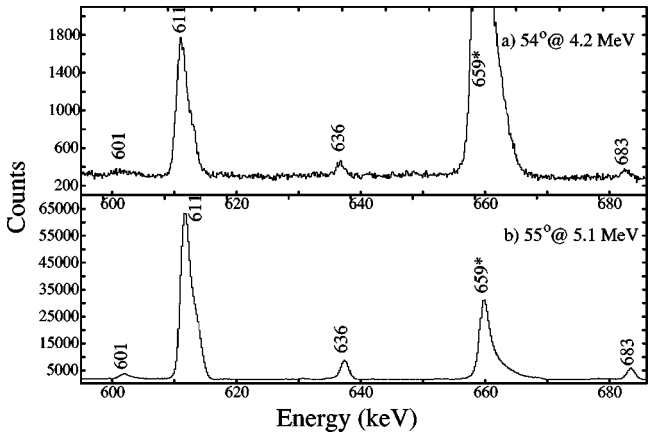

FIG. 2. Gamma-ray spectra obtained with (a) 4.2 MeV ^{3}He ions at 54° and (b) 5.1 MeV ^{3}He ions at 55°, showing the relative strengths of transitions directly feeding and indirectly depopulating the first $2^+_{T=1}$ state at 1586 keV. 11% of the deexcitation intensity of the 1586 keV level was measured as coming from observed higher-lying levels at $E_{^3\mathrm{He}}$=4.2 MeV, whereas 29% was measured for the 5.1 MeV experiment. The 659 keV γ ray (asterisk) is a doublet arising from ^{41}Ca and ^{18}F.

recoiling ^{42}Sc nuclei in the ^{40}Ca target. It implies the determination of the stopping matrix $P_\theta(t,v_\theta)$ which represents the normalized distributions of the recoil velocity projections v_θ (at a given angle θ with respect to the beam axis) as a function of the time t. The matrix is calculated by means of a Monte Carlo simulation where the nuclear and electron stopping powers, cross section of the reaction, reaction kinematics, detector resolution (FWHM), the finite size of the detector (solid angle) and proton emission spectra are taken into account (for more details, including the derivation of the stopping powers employed, see Ref. [14]). Correct inclusion of the proton emission effects has been found to be essential in order to reproduce the DSA line shapes. Depending on the direction of the emitted charged particles the linear momenta added to the recoils lead to a modification of their velocity distribution. Correspondingly, the observed Doppler-shift $E'_\gamma - E_{\gamma_0} = E_{\gamma_0}\langle v_\theta/c\rangle$ of the γ-ray energies is also modified. The measured singles spectrum or line shape is given by

$$S_{ij}(E_\gamma) = \int_{-\infty}^{\infty} \frac{c}{E_{\gamma_0}} \Phi(E'_\gamma, E_\gamma) dE'_\gamma \times \int_0^{\infty} P_\theta[t, v_\theta(E'_\gamma)] b_{ij} \lambda_i n_i(t) dt, \quad (7)$$

where n_i is the population of the level i as a function of the time t, λ_i is the decay constant of the level, and b_{ij} is the branching of the deexciting transition $i \rightarrow j$. Solving Eq. (7) with respect to the decay function $b_{ij}\lambda_i\, n_{i(t)}$ of the transition $i \rightarrow j$ can be used to extract the lifetime $\tau_i = 1/\lambda_i$ of the level of interest i. For this purpose, the population of the level of interest is represented by its natural form following from the solution of the Bateman equations for a system of radioactively decaying levels, namely $n_i(t) = \Sigma_{k \geqslant i} C_{ik} e^{-\lambda_k t}$. The sum includes all levels which feed directly or indirectly the level i. The coefficients C_{ik} depend on the initial population of the levels in the cascade, the branching ratios, and the decay constants λ_k. The fit consists in changing these quantities until the best description of the line shape is obtained, i.e., when the reduced χ^2 reaches a minimum.

It was found sufficient to describe the feeding of the $2^+_{T=1}$ level by two cascades. One of the cascades is slow, with an effective feeding time of a few picoseconds. Its inclusion was necessary for the reproduction of the stopped part of the line shape. The second cascade is extremely fast and leads to an almost direct population of the level of interest after the proton emission. The fitted relative intensities of both cascades are comparable at 4.2 MeV, but for the incident beam energy of 5.1 MeV the prompt cascade amounts already to about 60%.

IV. RESULTS

Figure 3 shows fits to the line shape of the 975 keV transition depopulating the first $2^+_{T=1}$ state at 1586 keV and observed in the 4.2 MeV experiment. This strong γ ray is detected as a single peak and displays line shapes dependent on the different angles measured. Figure 4 shows the fits to the line shape of the same transition for the incident beam energy of 5.1 MeV. The derived lifetimes τ here, which are also indicated in the figure, are systematically a bit smaller than those determined at 4.2 MeV. This discrepancy comes to some extent as a consequence of the proton emission effect which is stronger at 5.1 MeV. In addition, the increasing level density at higher excitation energies in ^{42}Sc and the larger cross section of the reaction complicates the correct determination of the lifetime at the higher beam energy. These problems are illustrated by the relatively large χ^2 values of the fits displayed in Fig. 4, although they may also be due to very low statistical errors per point. The results from both experiments are consistent and can be combined to yield the average value $\langle\tau\rangle = 69(18)$ fs for the lifetime from all fits. The uncertainty of 18 fs includes the statistical error, $\sigma = [(1/N-1)\Sigma(\tau - \langle\tau\rangle)^2]^{1/2}$, and an estimated 10% systematic error associated with the incomplete knowledge of the feeding and the stopping powers. This lifetime, together with a previous measurement of the branching ratio of the 975 and 1586 keV transitions as 100.0 ± 1.1 and 9.5 ± 1.1, respectively [19], leads to a value for the isoscalar matrix element of $M_0 = 6.8(8)$ W.u. As noted earlier, the previously determined lifetime of 100(30) fs and the same branching ratio measured by Kikstra *et al.* [19] lead to $M_0 = 5.7(9)$ W.u.

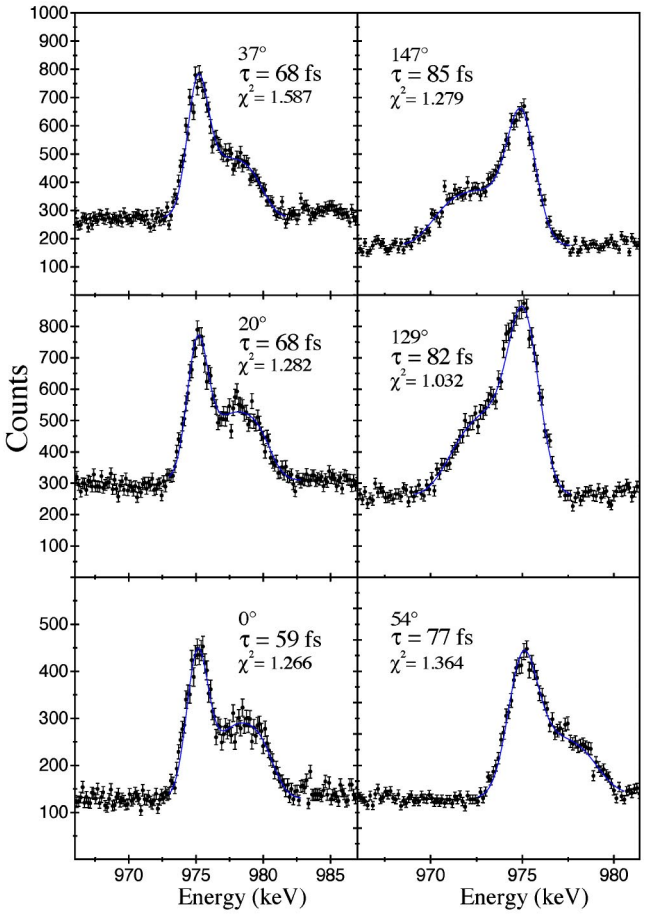

FIG. 3. (Color online) Lifetime determination by line-shape analysis of the 975 keV γ ray at $E_{^3\mathrm{He}} = 4.2$ MeV.

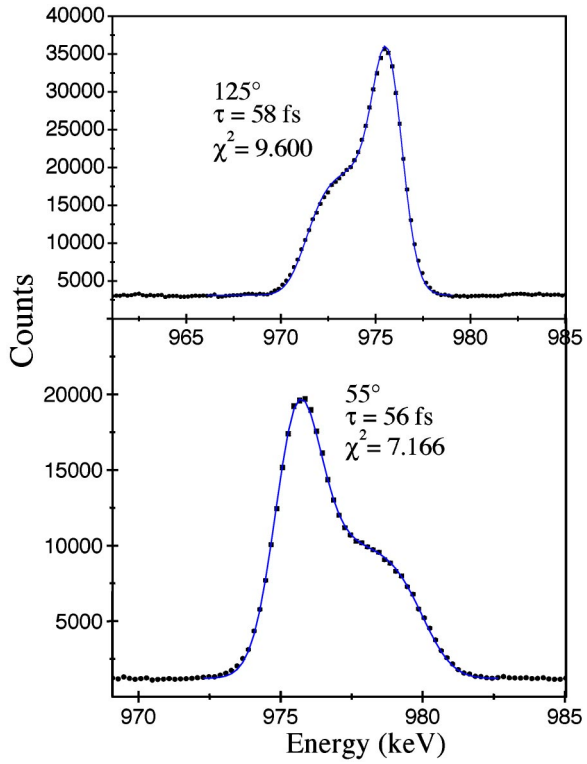

FIG. 4. (Color online) Line-shape analysis of the 975 keV γ ray from the $2^+_{T=1}$ at 1586 keV for the measurement with 5.1 MeV ^{3}He ions.

V. CONCLUSION

Figure 5 shows the isoscalar matrix elements for isobaric analogs from $A=22$ and up to the $A=42$ region. A comparison of the isoscalar matrix element obtained in the current work with that given by the mirror nuclei [5] indicates that isospin purity is conserved for the $A=42$ nuclei. It has to be mentioned that the side feeding is taken into account on the basis of theoretical predictions given by PACE2, and is expected that a future experiment measuring the proton distribution of the $(^3\mathrm{He},p)$ reaction at 4.2 and 5.1 MeV will test these theoretical predictions. Finally, the systematics of the isoscalar matrix elements from $A=22$ to $A=38$ shows a particular decreasing trend when approaching the $Z=N=20$ closed shell, whereas the trend seems to be broken when the $f_{7/2}$ shell begins to be filled in the $A=42$ isobars.

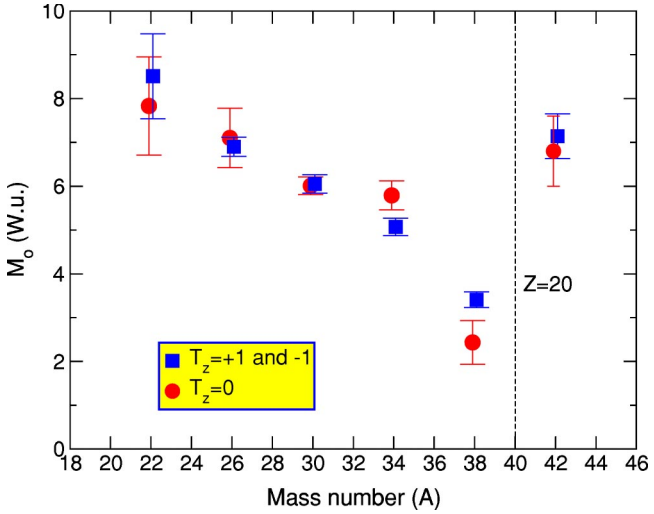

FIG. 5. (Color online) Isoscalar multipole matrix elements as a function of the mass number for the first 2^+ ($T=1$) to 0^+ ($T=1$) transition. This comparison was developed in Ref. [5]; our work shows the isoscalar matrix element for the $T_Z=0$ nucleus, ^{42}Sc (circle point), in the $A=42$ isobars.

ACKNOWLEDGMENTS

This work was supported by the U.S. National Science Foundation under Grant Nos. PHY-0098813 and PHY-0354656.

[1] E. Feenberg and E. P. Wigner, Phys. Rev. **51**, 95 (1937).
[2] M. A. Bentley, C. D. O'Leary, A. Poves, G. Martinez-Pinedo, D. E. Appelbe, R. A. Bark, D. M. Cullen, S. Erturk, and A. Maj, Phys. Lett. B **437**, 243 (1998).
[3] M. A. Bentley, S. J. Williams, D. T. Joss, C. D. O'Leary, A. M. Bruce, J. A. Cameron, M. P. Carpenter, P. Fallon, L. Frankland, W. Gelletly, C. J. Lister, G. Martinez-Pinedo, A. Poves, P. H. Regan, P. Reiter, B. Rubio, J. Sanchez Solano, D. Seweryniak, C. E. Svensson, S. M. Vincent, and D. D. Warner, Phys. Rev. C **62**, 051303 (2000).
[4] A. M. Bernstein, V. R. Brown, and V. A. Madsen, Phys. Rev. Lett. **42**, 425 (1979).
[5] P. D. Cottle, M. Fauerbach, T. Glasmacher, R. W. Ibbotson, K. W. Kemper, B. Pritychenko, H. Scheit, and M. Steiner, Phys. Rev. C **60**, 031301 (1999).
[6] P. D. Cottle, Z. Hu, B. V. Pritychenko, J. A. Church, M. Fauerbach, T. Glasmacher, R. W. Ibbotson, K. W. Kemper, L. A. Riley, H. Scheit, and M. Steiner, Phys. Rev. Lett. **88**, 172502 (2002).
[7] L. A. Riley, P. D. Cottle, M. Brown-Hayes, W. T. Cluff, J. D. Fox, N. Keeley, F. W. Letson, R. A. Kaye, K. W. Kemper, M. T. McEllistrem, S. L. Tabor, J. M. Thompson, and D. Walker, Phys. Rev. C **68**, 044309 (2003).
[8] A. G. Sitenko and V. K. Tartakovskii, in *Lectures on the Theory of the Nucleus*, edited by P. J. Shepherd (Pergamon, New York, 1975), pp. 11–24.
[9] T. Glasmacher, Annu. Rev. Nucl. Part. Sci. **48**, 1 (1998).
[10] B. Heusch and A. Gallmann, Phys. Rev. C **7**, 1810 (1973).
[11] J. Hazan and G. Merkel, Phys. Rev. **139**, B835 (1965).
[12] D. P. Balamuth, G. P. Anastassiou, and R. W. Zurmuhle, Phys. Rev. C **2**, 215 (1970).
[13] G. Böhm, A. Dewald, P. Petkov, and P. von Brentano, Nucl. Instrum. Methods Phys. Res. A **329**, 428 (1993).
[14] P. Petkov, J. Gableske, O. Vogel, A. Dewald, P. von Brentano, R. Krücken, R. Peusquens, N. Nicolay, A. Gizon, J. Gizon, D. Bazzacco, C. Rossi-Alvarez, S. Lunardi, P. Pavan, D. R.

Napoli, W. Andrejtscheff, and R. V. Jolos, Nucl. Phys. **A640**, 293 (1998).

[15] N. R. Roberson and G. van Middelkoop, Nucl. Phys. **A176**, 577 (1971).

[16] M. T. McEllistrem, in *Nuclear Research with Low Energy Accelerators*, edited by J. B. Marion and D. M. Van Patter (Academic, New York, 1967), p. 167; P. E. Garrett, N. Warr, and S. W. Yates, J. Res. Natl. Inst. Stand. Technol. **105**, 141 (2000).

[17] Projection Angular-Momentum Evaporation Code for Fusion-Evaporation Reaction, University of Liverpool, 2003.

[18] D. Tonev, P. Petkov, A. Dewald, T. Klug, P. von Brentano, W. Andrejtscheff, S. M. Lenzi, D. R. Napoli, N. Marginean, F. Brandolini, C. A. Ur, M. Axiotis, P. G. Bizzeti, and A. Bizzeti-Sona, Phys. Rev. C **65**, 034314 (2002).

[19] S. W. Kikstra, C. van der Leun, S. Raman, E. T. Jurney, and I. S. Towner, Nucl. Phys. **A496**, 429 (1989).